Silver Nanowire Percolation Network Soldered with Graphene Oxide at Room Temperature and Its Application for Fully Stretchable Polymer Light-Emitting Diodes

Jiajie Liang,[†,§] Lu Li,[†,§] Kwing Tong,[†] Zhi Ren,[†] Wei Hu,[†] Xiaofan Niu,[†] Yongsheng Chen,[‡] and Qibing Pei[†,*]

[†]Department of Materials Science and Engineering, Henry Samueli School of Engineering and Applied Science, University of California, Los Angeles, California 90095, United States and [‡]Key Laboratory of Functional Polymer Materials and Centre of Nanoscale Science and Technology Institute of Polymer Chemistry, College of Chemistry, Nankai University, 300071 Tianjin, China. [§]J.L. and L.L. contributed equally.

ABSTRACT Transparent conductive electrodes with high surface conductivity, high transmittance in the visible wavelength range, and mechanical compliance are one of the major challenges in the fabrication of stretchable optoelectronic devices. We report the preparation of a transparent conductive electrode (TCE) based on a silver nanowire (AgNW) percolation network modified with graphene oxide (GO). The monatomic thickness, mechanical flexibility, and strong bonding with AgNWs enable the GO sheets to wrap around and solder the AgNW junctions and thus dramatically reduce the inter-nanowire contact resistance without heat treatment or high force pressing. The GO-soldered AgNW network has a figure-of-merit sheet resistance of 14 ohm/sq with 88% transmittance at 550 nm. Its storage stability is improved compared to a conventional high-temperature annealed AgNW network. The GO-soldered AgNW network on polyethylene terephthalate films was processed from solutions using a drawdown machine at room temperature. When bent to 4 mm radius, its sheet resistance was increased by only 2−3% after 12 000 bending cycles. GO solder can also improve the stretchability of the AgNW network. Composite TCE fabricated by inlaying a GO-soldered AgNW network in the surface layer of polyurethane acrylate films is stretchable, by greater than 100% linear strain without losing electrical conductivity. Fully stretchable white polymer light-emitting diodes (PLEDs) were fabricated for the first time, employing the stretchable TCE as both the anode and cathode. The PLED can survive after 100 stretching cycles between 0 and 40% strain and can be stretched up to 130% linear strain at room temperature.

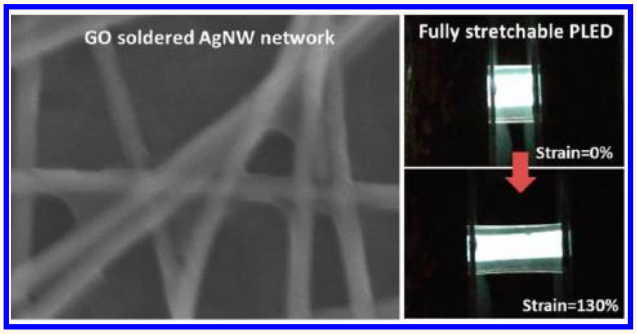

KEYWORDS: transparent conductive electrode · stretchable · silver nanowires · graphene oxide · light-emitting diode

Transparent conductive electrode (TCE) has become a focus of considerable research activities in recent years since it is an essential material in various optoelectronic devices, such as thin film solar cells, liquid crystal displays, organic light-emitting diodes, and touch sensing panels. The rapidly growing interests in recent years for flexible and stretchable optoelectronics have posed a major materials challenge to develop a TCE with mechanical flexibility or even rubbery stretchability.[1−6] Indium tin oxide (ITO) has been the ubiquitous TCE material.[7] However, high-quality ITO coating can only be obtained *via* high-temperature annealing. ITO coating formed on flexible substrates such as polyethylene terephthalate (PET) has higher sheet resistance than ITO formed on glass, and its flexibility is limited due to the brittleness of the ceramic coating.[8] Several alternative materials, including carbon nanotubes (CNTs),[5,9−15] graphene,[16−19] and conducting polymers,[20−22] have been investigated to replace ITO with varied successes. It has been shown that the deformation of CNT networks and buckling can allow large-strain deformation without

* Address correspondence to qpei@seas.ucla.edu.

Received for review November 13, 2013 and accepted January 28, 2014.

Published online January 28, 2014
10.1021/nn405887k

much increase of surface conductivity.[3,5,11−14] These carbon or polymer-based materials have relatively low electrical conductivity, and the sheet resistances of corresponding TCE are 1−2 orders of magnitude higher than that of ITO/glass.[17,23] Percolation networks of silver nanowires (AgNWs) have shown promise to rival ITO/glass in sheet resistance and visual transparency.[24−27] Due to the high conductivity of silver, the sheet resistance of a AgNW percolation network is dominated by the contact resistance of inter-nanowire junctions.[28,29] Postprocessing treatments, such as high-temperature annealing (normally higher than 180 °C),[24,30,31] high-force pressing,[26,32−34] and plasmonic welding,[28] are effective in reducing the junction resistance by fusing the AgNW junctions. A number of works have employed AgNW networks to fabricate stretchable TCE.[23,35−39] However, the stretchability of these AgNW networks is limited because, under large tensile deformation, the nanowire junctions could detach and the nanowires slide against each other to cause high contact resistance that cannot be fully recovered when the stretched material is relaxed to its original shape.

Introducing a second functional component into the AgNW network to forge inter-nanowire connection has been reported as a promising technique to reduce the sheet resistance of AgNW networks.[40−43] Lee *et al.* used poly(3,4-ethylenedioxythiophene):poly(styrenesulfonate) (PEDOTE:PSS) as a soldering material to make a AgNW/PEDOT:PSS hybrid composite electrode.[41] The stretchability of this hybrid electrode is relative low, and the PEDOT:PSS could uptake environmental water and cause corrosion of the AgNWs.[42] During the preparation of this article, Lee *et al.* reported integrating AgNW networks onto chemical vapor deposited (CVD) graphene to make a graphene−AgNW hybrid that exhibits high optical-electrostretchable performance.[43] This approach does not appear to be compatible with large-area, low-cost processing that has been one of the major motivations for using the AgNW-based TCE.

Herein, we report the preparation of a highly conductive AgNW and graphene oxide (GO) hybrid network by all-solution processing at room temperature. GO, a monatomic layer thick two-dimensional material, was chosen as a soldering material for AgNW junctions based on the following considerations: (1) GO contains a large number of oxygen-containing groups, such as hydroxyl, epoxide, diol, ketone, and carboxyl, that could forge strong bonding with AgNWs; (2) it has an extremely high Young's modulus (~0.25 TPa) and a high flexibility, making it an extremely tough material; and (3) GO is inexpensive and solution-processable.[44−47] The charged and flexible GO sheets in solution could adhere and wrap around the AgNWs and solder the inter-nanowire junctions, causing significant reduction of the inter-nanowire contact resistance without heat treatment or high-force pressing. The GO-AgNW network thus can be formed on polyethylene terephthalate (PET) with high optical-electrical performance and mechanical flexibility. The strong bonding and high toughness of GO could also knot-tie the AgNW networks to prevent inter-nanowire sliding and thus allow reversible large-strain deformation. Stretchable TCE based on the GO-soldered AgNW network inlaid in the surface layer of polyurethane acrylate (PUA) shows rubbery stretchability while retaining its high electrical conductivity. Furthermore, fully stretchable white polymer light-emitting diodes (PLEDs) have also been demonstrated for the first time using this stretchable TCE as both the anode and the cathode.

RESULTS AND DISCUSSION

The process to fabricate a GO-AgNW network, as illustrated in Figure 1a, started with bar-coating a layer of AgNWs on a glass substrate from a dispersion in isopropyl alcohol (IPA) using a drawdown machine. Figure 1b displays an optical photograph of an as-prepared AgNW network with 20 × 15 cm^2 area on a glass substrate. Sheet resistance and transmittance of the AgNW coating was determined by the coating density (mg/m^2) of the AgNW percolation network which is controlled *via* the concentration of the AgNW ink, as detailed in the Methods section. The dried AgNW coating was subsequently soaked into a 1 mg/mL GO dispersion in distilled water and IPA for several minutes without any heating or stirring. The AgNW coating was then rinsed with distilled water repeatedly and blow-dried. All of these procedures were solution-based and carried out at room temperature.

The microstructure of the resulting GO-AgNW network was imaged by scanning electron microscopy (SEM), as shown in Figure 1c. The AgNW junctions are wrapped and soldered by GO sheets. SEM image in Figure S1 (Supporting Information) further depicts that almost all the AgNW junctions in the network are soldered by GO sheets. The GO-soldered junctions are quite different from those fused through thermal heating (Figure 1d, 180 °C annealed for 30 min). The soldered junctions are also different from those using graphene or GO/AgNW hybrids, wherein the graphene or GO sheets covered like a blanket on top of the AgNW networks.[29,40,43,48] In our process, the soldering of AgNW junctions by GO is result of (1) the unique properties of GO, including various oxygen-containing functional groups present on the surface and the outstanding mechanical strength and flexibility, and (2) the process of soaking AgNW networks in a GO solution. When the AgNW networks are soaked in a GO dispersion, the charged GO sheets tend to bond with the AgNWs and AgNW junctions due to the strong electrostatic adhesion. The flexibility of the GO sheets allows them to conform around the AgNW junctions

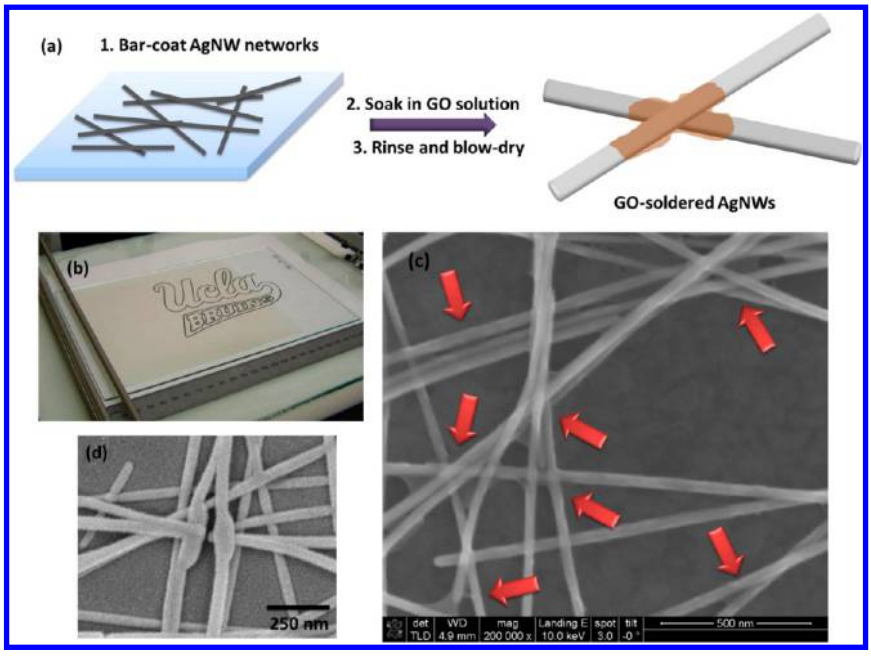

Figure 1. (a) Schematic illustration of the fabrication of a GO-AgNW network on a glass substrate at room temperature. (b) Optical photograph of a AgNW network (20 × 15 cm^2) bar-coated on a drawdown machine. SEM images of (c) GO-soldered AgNW junctions (indicated by red arrows) and (d) typical high-temperature fused AgNW junctions.

like a plastic wrap. The rinsing process washed off the GO sheets that do not bond strongly with AgNWs. Blow-drying the GO-AgNW coating facilitates the GO sheets to wrap around the AgNW junctions and knot-tie the junctions due to electrostatic forces as well as capillary force during the evaporation of solvent molecules between the GO and AgNWs. The GO sheets have high toughness and act as a soldering material when wrapped around the AgNW junctions. Knot-tying the AgNW junctions can not only reduce the inter-nanowire contact resistance but also prevent inter-nanowire sliding at the junctions. This will be further discussed below.

The sheet resistance of the GO-AgNW networks as a function of soaking time in GO solution is depicted in Figure 2a. The sheet resistance can be greatly lowered from 1045 to 26 and 20 ohm/sq after just 30 s and 1 min soaking time, respectively. In 5 min of soaking, the GO-AgNW network reaches a low sheet resistance of 14 ohm/sq. Prolonged soaking does not considerably lower the sheet resistance. In comparison, thermal treatment to fuse the AgNW junctions usually takes more than 30 min to complete.[24,30,31]

The sheet resistance and transparency of the GO-AgNW networks are dependent on the coating density of AgNWs. Figure 2b shows the results for three representative GO-AgNW networks with three AgNW densities: D1, 85 mg/m^2; D2, 127 mg/m^2; and D3, 170 mg/m^2. Their sheet resistance and transmittance at 550 nm are 26, 14, and 12 ohm/sq and 92.1, 88.2, and 86.0%, respectively. Figure 2c compares the optical-electroperformance of the GO-AgNW networks with important TCEs published in the literature and commercial ITO. It can be seen that the GO-AgNW networks fabricated through solution-based process at room temperature conditions exhibit comparable electro-optical performance to commercial ITO coated on glass, significantly higher performance than ITO/PET (a commercial material widely used for flexible optoelectronic devices), and higher performance than most of the new TCE intended to replace ITO. Furthermore, the GO-AgNW networks are also superior to most thermally treated or hot-pressed AgNW networks, and the only AgNW network that exhibits lower sheet resistance with higher transmittance is that made up of nanowires with extremely long length.[27]

Supporting Information Figure S2 shows the transmittance spectra of AgNW networks with three different coating densities, D1, D2, and D2, treated by either GO soldering (GO-AgNW) or high-temperature annealing at 180 °C for 30 min (named HT-AgNW; the annealing condition was optimized in our previous study).[30,31,39] At the same AgNW densities, GO-AgNW and HT-AgNW networks show almost identical transmittance. This result indicates that there are little GO sheets located in the optical pathway unblocked by AgNWs; that is, almost all GO sheets present in the coating wrap around the AgNWs and AgNW junctions and add little to total optical loss of the coating. This analysis is consistent with the SEM observation shown in Figure 1c. The GO-AgNW networks are different from the reported CVD graphene/AgNW coatings where the graphene sheets cover the AgNW network like a blanket.[41]

Figure 3a compares the sheet resistance of GO-AgNW and HT-AgNW networks at the same AgNW

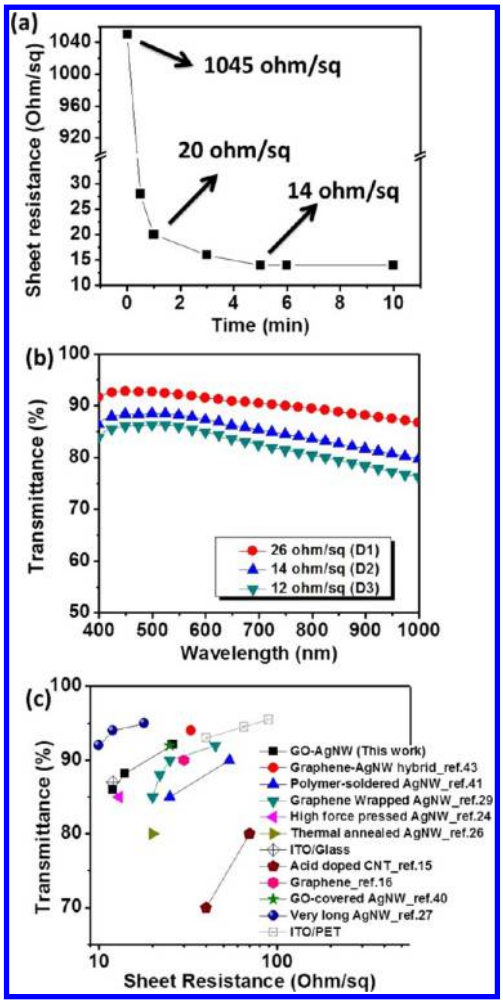

Figure 2. (a) Measured sheet resistance of a GO-AgNW network as a function of the soaking time in a GO solution. (b) Transmittance spectra of GO-AgNW networks with three different AgNW densities (D1, D2, and D3). (c) Comparison of the electro-optical performance of the GO-AgNW networks with various TCE films published in the literature and commercial ITO/glass and ITO/PET (all data are exclusive of substrate).

densities. One interesting trend to note is that, at low AgNW density (D1), GO-AgNW is more conductive than HT-AgNW. At high density (D3), HT-AgNW is more conductive. One plausible explanation is that, at low densities, AgNWs are sparsely distributed. The binding force of GO helps move nearby AgNWs to form low resistance joints. At high AgNW density, AgNW junctions are abundant, and the fusing between AgNWs becomes much more effective to lower the junction resistance than GO soldering does without thermal treatment.

The GO-AgNW and HT-AgNW networks show different storage stability. Figure 3b displays the resistance change of the networks during accelerated test at 85 °C in air. The sheet resistance of the HT-AgNW network increases by 5% in 1 day. Longer heating up to 8 days total does not further increase the resistance. In contrast, the sheet resistance of the GO-AgNW

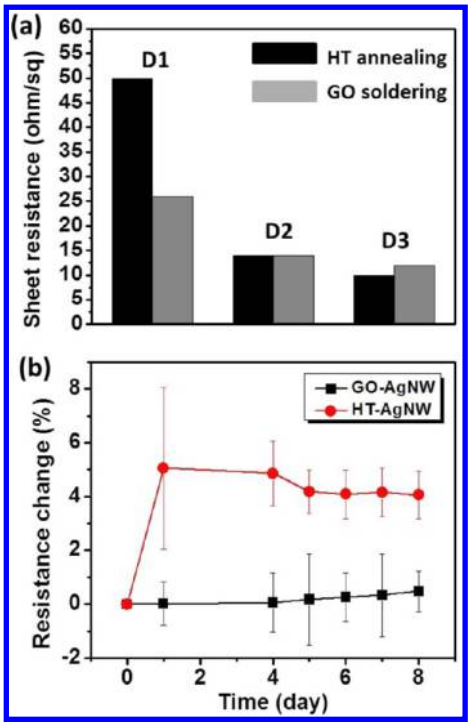

Figure 3. (a) Comparison of sheet resistance of GO-AgNW networks with HT-AgNW networks. (b) Plots of the relative sheet resistance change *versus* time for GO-AgNW networks and HT-AgNW networks with the same AgNW densities (D2) after exposure to hot air (85 °C) for 8 days.

network increases by a mere ~0.4% in 8 days. The sheet resistance increase of AgNW networks has been reported in the literature and attributed to attacks by environmental oxygen and sulfur which can significantly increase the junction resistance.[40,43] Graphene sheets have been shown to be an excellent barrier material. We suggest that GO wrapping around the AgNW junctions can impede the environmental oxidants from oxidizing the AgNWs and their junctions and increase the stability for the GO-AgNW networks.

ITO coated on PET is widely used in industry for flexible optoelectronic devices. The flexibility of ITO/PET films are rather limited; strain of 1% or larger can cause irreversible crack formation in the ITO.[31] AgNW network coated on a plastic substrate is a widely investigated alternative material. However, the conventional approach of fusing AgNWs at elevated temperatures is only applicable to high-temperature substrates. The solution-based room temperature processing allows the formation of GO-AgNW networks on much more polymer-based substrates, such as PET, polyethylene naphthalate, and polyacrylate. Figure 4a displays a sheet of GO-AgNW/PET with an area of 20×40 cm^2 and sheet resistance of 26 ± 5 ohm/sq (the error range indicates the variation of local sheet resistance and is insignificant for most applications). Mechanical flexibility of a GO-AgNW/PET film was evaluated by repeated bending to a radius of 4 mm using a linear stretcher built in house (Figure 4b). The

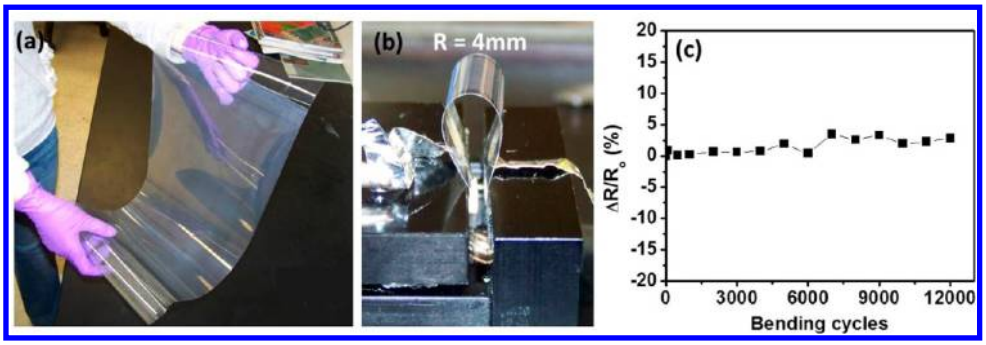

Figure 4. (a) Optical photograph of a GO-AgNW/PET sheet (26 ohm/sq) coated on a drawdown machine (coating area: 20 × 40 cm^2). (b) Optical photograph of a GO-AgNW/PET bent to 4 mm radius. (c) Relative resistance change of the GO-AgNW/PET during repeated bending−unbending test (bending radius: 4 mm).

moving speed of the stretcher was set at 50 mm/s. During 12 000 cycles of bending−unbending, the resistance of the GO-AgNW network remained relatively stable (Figure 4c). It increased by merely 2−3%, revealing good flexibility of the GO-AgNW network. Moreover, this GO-AgNW/PET (26 ohm/sq) also shows better electro-optical performance than the commercial ITO/PET film (35 ohm/sq, obtained from Aldrich), as shown in Figure S3.

The GO-AgNW networks were also employed to fabricate a stretchable transparent composite electrode by an *in situ* substrate polymerization and transfer technique that we have previously reported for HT-AgNW networks.[5,37,49] A urethane acrylate monomer was coated onto the GO-AgNW network on a releasing glass substrate. The monomer was cured, and the resulting PUA film was peeled off to transfer the GO-AgNW network into the surface layer of the PUA film. Figure 5a shows the transmittance spectra of the GO-AgNW/PUA composite electrodes with three AgNW densities (D1, D2, and D3). The transmittance at 550 nm is 86.3, 82.5, and 79.2% for composite electrodes with sheet resistances of 26, 14, and 12 Ω/sq, respectively. It should be noted that the transmittance data are inclusive of the PUA matrix, while the data reported in many published papers are for AgNW coating only. In order to test the stretchability of the transparent composite electrodes, samples with dimensions of 20 mm in length and 5 mm in width were mounted on a motorized linear stage, leaving a 5 mm length (gauge length) free to deform. All samples were stretched at 1 mm/s (strain rate: 20%/s), and the resistance was monitored in sync with the stretching. Figure 5b displays the normalized resistance (R/R_0, the ratio of the instantaneous resistance at a specific tensile strain to the initial resistance at zero strain) for the GO-AgNW/PUA and HT-AgNW/PUA composite electrodes. Both electrodes have the same AgNW densities (D2) and the same initial sheet resistance (14 ohm/sq). More than five samples of each electrode were tested, and the variation of resistance among the samples in each group was within ±10%. The GO-AgNW/PUA electrode shows much smaller resistance

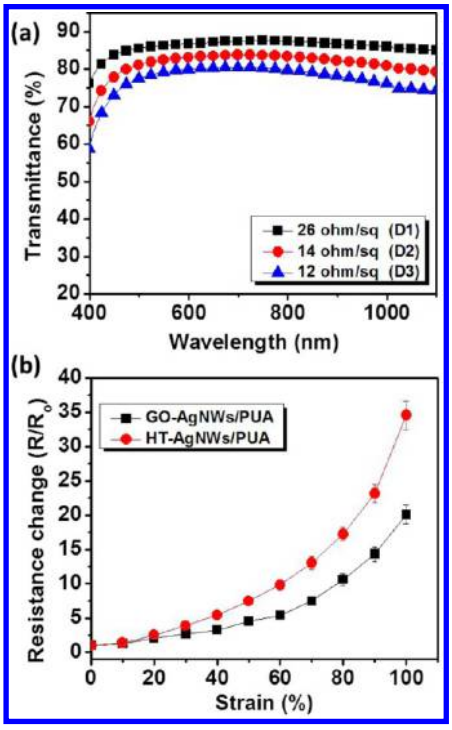

Figure 5. (a) Transmittance spectra of GO-AgNW/PUA composite electrodes with specified sheet resistance. (b) Normalized resistance of the 14 ohm/sq GO-AgNW/PUA composite electrodes and 14 ohm/sq HT-AgNW/PUA composite electrodes as a function of tensile strain (strain rate is 1 mm/s).

increase with strain than the HT-AgNW/PUA electrode. The resistance increase of the GO-AgNW/PUA is 3.2-, 5.3-, and 10.6-fold at strains of 40, 60, and 80%, respectively; in comparison, the increase is 5.4, 9.8, and 17.2, respectively, for the HT-AgNW/PUA.

The difference in stretchability between the GO-AgNW/PUA and HT-AgNW/PUA is also shown in repeated stretching−relaxing (Figure 6a,b). During 100 cycles of stretching−relaxing between 0 and 20% strains, the peak of the resistance change (at 20% strain) for GO-AgNW/PUA increases very gradually from about 2.3 to 2.7 times its initial value; as for the HT-AgNW/PUA, the peak resistance increases from 2.9 to 3.3 times its initial value. During the cyclic tests

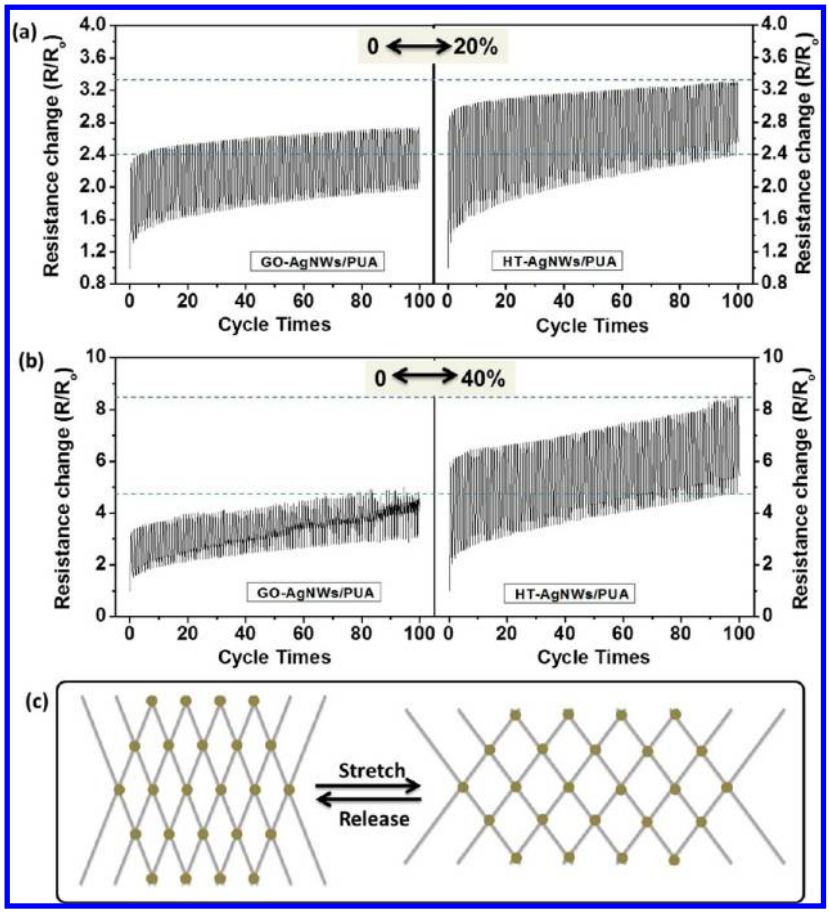

Figure 6. Normalized transient resistance of GO-AgNW/PUA and HT-AgNW/PUA composite electrodes during 100 cycles of tensile stretching and releasing between 0 and 20% strains (a) and 0 and 40% strains (b). The initial sheet resistances of both electrodes are 14 ohm/sq. The stretching speed is 1 mm/s. (c) Schematic illustration of the deformation of an ideal nanowire network wherein the nanowire junctions are intact during uniaxial stretching.

between 0 and 40% strain, the peak resistance of GO-AgNW/PUA increases from about 3.4 to 4.8 times its initial value in 100 cycles, while that of the HT-AgNW/PUA increases from 6.0 to 8.5 times its initial value. The results indicate fairly high stretching reversibility for both electrodes, but the GO-AgNW/PUA clearly shows higher stability as indicated by the smaller width of the ribbons (the shaded area formed between the peak and trough resistances in Figure 6a,b).

For bulk conductive material, its resistance increases with strain following the equation $R/R_0 = (1 + \text{strain})^2$ due to geometrical changes (elongation in length and shrinking in width due to Poisson's law).[38,50,51] For an ideal network formed by conductive nanowires in which the nanowire junctions are intact during stretching, like a fishnet (Figure 6c), the geometrical changes during a uniaxial stretching should not cause any significant resistance increase. The macroscopic elongation of the network would cause stress around the junctions and possible buckling or twisting of the nanowires. The corresponding change in macroscopic resistance should be small as the conduction pathways along the nanowires remain more or less the same. The loss of surface conductivity of HT-AgNW networks under large tensile strain has been considered to be caused in large by the loss of interconnection between the nanowires.[23] The thermal-fused AgNW junctions may be easily broken under twisting stress. Embedding the HT-AgNW networks in an elastomeric matrix, such as in the composite electrodes of HT-AgNW/PUA, can limit the degree of junction disjointing and nanowire sliding.[35,38,39,49] The elastomeric matrix can help distribute the stress more uniformly. In the GO-AgNW/PUA composite electrode, wrapping of the junctions by the flexible yet very tough GO sheets can allow the twist of GO-soldered AgNW junctions and prevent the disjointing or sliding of AgNW nanowires against each other during large-strain deformation. Stretchability of the GO-AgNW networks is thus improved. However, compared to the fishnet model in Figure 6c, the silver nanowires are not sufficiently stretchable and tough. Large-strain deformation can still cause macroscopic resistance increase, and some of the increase is irreversible, and disjointing, sliding, and even fracture could still occur, albeit at a smaller extent compared to what has been reported in literature.[37−39,41]

We have reported the fabrication of fully stretchable polymer light-emitting electrochemical cells (PLEC) by

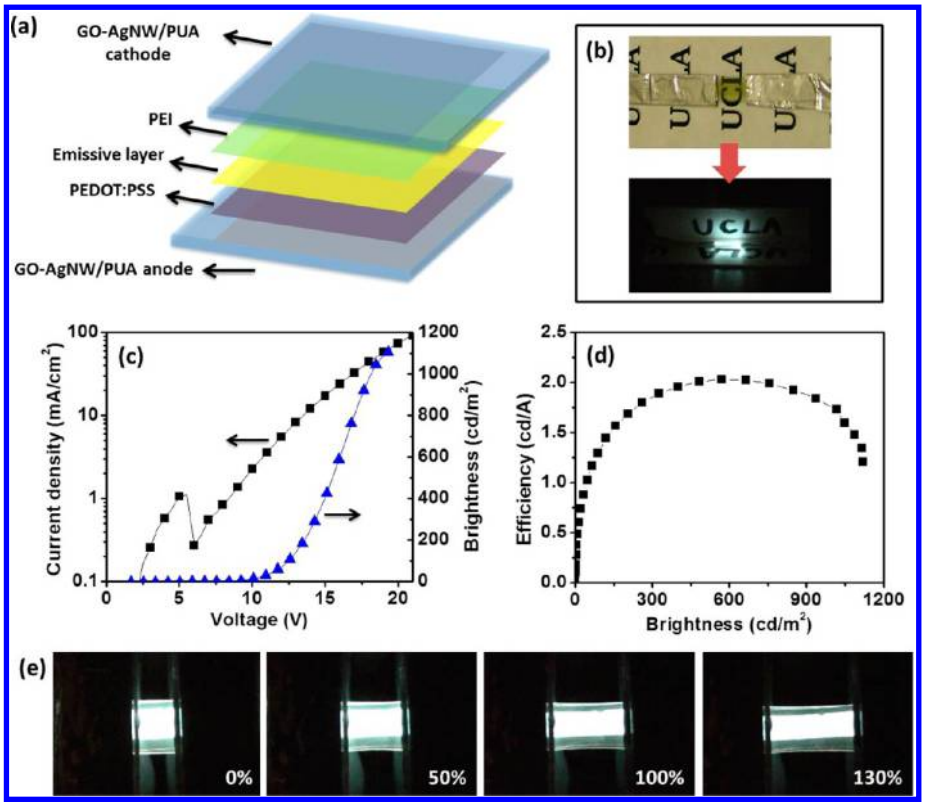

Figure 7. (a) Schematic drawing of a fully stretchable PLED using GO-AgNW/PUA composite electrode as both anode and cathode. (b) Optical photographs of a semitransparent unlit stretchable PLED (top) and a stretchable PLED operated at 13 V emitting white light from two sides and illuminating two white papers with printed ULCA logo in black (bottom). (c) Current density−luminance−driving voltage characteristics and (d) current efficiency−brightness characteristics of the PLED device. (e) Optical photographs of a PLED (original lighting area: 3 mm × 4 mm) being driven at 14 V and stretched to specified strains.

sandwiching a thin film of a blend of luminescent conjugated polymer, an ionic conductor, and lithium salt between a pair of composite electrodes.[5,49] The composite electrodes comprise a thin percolation network of HT-AgNWs or SWCNTs in the surface layer of the polymer substrate. With the use of shape memory polymer or elastomeric polymer as the substrate, the PLECs are fully stretchable, wherein all components are elongated as the thin film devices are stretched.[5,6,49] These stretchable PLECs suffer from such problems as slow turn-on and short lifetime at high brightness that are quite characteristic for PLECs.[52,53] To evaluate the application potential of the GO-AgNW/PUA composite electrode for fully stretchable white PLED, the electroluminescence of which does not require the *in situ* formation of a p-i-n junction as in the PLECs, light-emitting diodes were fabricated by solution-based coating and lamination process. Atom force microscope measurement showed that the height variation of the GO-AgNW/PUA composite electrode surface is around 10 nm (Figure S4), which is suitable for the fabrication of a PLED. The devices have a thin film sandwich structure of GO-AgNW/PUA/poly(3,4-ethylenedioxythiophene):poly(styrenesulfonate) (PEDOT:PSS)/emissive polymer layer/polyethylenimine (PEI)/GO-AgNW/PUA, as illustrated in Figure 7a. In a nutshell, the solution-based fabrication process started spin-coating a PEDOT:PSS layer on GO-AgNW/PUA as the hole transporting layer (HTL); the emissive layer (EL), consisting of a white-light-emitting polymer and 1,3-bis[(4-*tert*-butylphenyl)-1,3,4-oxidiazolyl]phenylene (OXD-7) mixed at weight ratio of 100:10, was then spin-coated on top of the HTL. On a second GO-AgNW/PUA, polyethylenimine (PEI), 5 nm thick, was coated as the electron transporting layer (ETL) to enhance electron injection.[54] The two GO-AgNW/PUA films were laminated with the conductive layers facing each other. The sheet resistance of the GO-AgNW/PUA composite electrodes used was 14 ohm/sq. These materials were selected for stretchability of the resulting PLEDs. The composition and layer thickness were preliminarily optimized for overall performance in electroluminescent and stretchability.

The characteristic current density−brightness−driving voltage responses ($J-B-V$) and current efficiency−brightness curves ($\eta-L$) of the PLED are measured as shown in Figure 7c,d. Leakage current can be seen from 1 to 6 V in the $J-B-V$ curve, which could be caused by the surface roughness of composite electrodes or defects introduced during the lamination process. The electroluminescence turns on at around 7 V and reaches a brightness of 1100 cd/m^2 at 21 V. The maximum current efficiency is 2.0 cd/A obtained at the brightness of 571 cd/m^2. Figure 7b shows an undriven

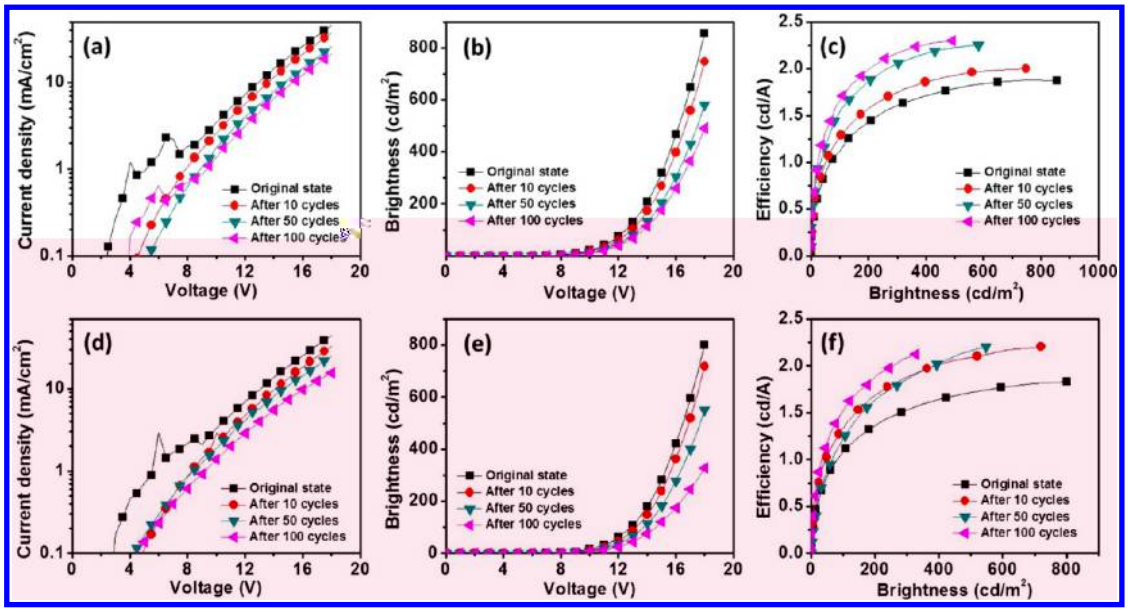

Figure 8. (a) Current density−driving voltage, (b) brightness−driving voltage, and (c) current efficiency−brightness characteristics of a stretchable PLED after specified stretching−relaxing cycles between 0 and 20% strains. (d) Current density−driving voltage, (e) brightness−driving voltage, and (f) current efficiency−brightness characteristics of a stretchable PLED after specified stretching−relaxing cycles between 0 and 40% strains.

semitransparent PLED and a driven PLED emitting white light from both sides. The light emitted from either side of the transparent PLED has almost identical $J-B-V$ and $\eta-L$ responses, as shown in Figure S5. Therefore, the actual emission intensity and efficiency of the PLEDs are twice as much as shown in Figure 7, and the maximum current efficiency is 4.0 cd/A.[49,55]

The CIE coordinates of the emission color are depicted in Figure S6 on the Commission Internationale de L'Eclairage (CIE) 1931 chromaticity coordinates diagram. At the emission brightness of 100, 500, and 1000 cd/m^2, measured from one side of the devices, the color coordinates are (0.35, 0.35), (0.33, 0.34), and (0.31, 0.34), respectively, all being fairly close to pure white (0.33, 0.33). More importantly, the PLEDs are soft and stretchable at room temperature. As shown in Figure 7e, the PLED with a lighting area of 3 $\times$ 4 cm^2 can be stretched by as large as 130% linear strain while driven at 14 V. The emission intensity is fairly uniform across the entire lit area.

The supplementary video clip (Supporting Information) demonstrates stretching operation of a PLED and shows a fairly uniform and bright light emission during stretching−releasing cycles. Figure 8 demonstrates the current density−driving voltage ($I-V$), brightness−driving voltage ($B-V$), and current efficiency−brightness ($\eta-B$) characteristic curves of PLED after 10, 50, and 100 cycles of stretching−relaxing between 0 and 20% strains (Figure 8a−c) and between 0 and 40% strains (Figure 8d−f). The leakage current, which is clearly seen from the $I-V$ curves for the original PLEDs, is largely suppressed after the stretching−releasing cycles. The brightness−voltage and current efficiency−brightness curves both exhibit a declining trend with increasing stretching−releasing cycles. However, the turn-on voltage of the stretched PLEDs does not change much with stretching−releasing cycles. The current efficiency gradually increases with each additional stretching−releasing cycle. For instance, for a fresh PLED with a current efficiency of 1.5 cd/A at 280 cd/m^2, its current efficiency is increased to 2.1 cd/A at the same brightness after 100 cycles of stretching−releasing between 0 and 40%. This increasing efficiency may be consistent with the decreasing leakage current. There could be other factors that could affect the efficiency of the stretchable PLEDs after stretching. Charging injection interfaces, thickness of the emissive layer, molecular orientation, and morphological changes could all play an important role in the electroluminescence. Substantial efforts are required to fully optimize the mechanical and electroluminescent properties of the PLEDs.

CONCLUSIONS

In summary, the GO sheet is a useful material to solder AgNW junctions. Immersing the AgNW coating in GO solutions leads to deposition of GO sheets to wrap around the nanowires and their junctions. There is little deposition of GO sheets in the substrate surface areas uncovered by the nanowires, which allow for the decrease in sheet resistance of the network without significant lost of optical transmittance. The highly conductive and transparent GO-AgNW networks could be formed on flexible substrates such as PET *via* an all-solution-based process at room temperature. The obtained GO-AgNW networks exhibit high mechanical

flexibility. When embedded in the surface layer of the elastomeric PUA, the transparent composite electrode behaves like a rubbery substance at room temperature. The films could be stretched repeatedly to 40% strains due to the strong bonding of the GO sheets on the junctions to prevent disjointing or sliding of the nanowires against each other during large-strain deformation. The rubbery composite electrode was used successfully to demonstrate, for the first time, fully stretchable polymer light-emitting diodes that could be stretched by as much as 130% and repeatedly by 40%. Large-strain deformation can cause a lot of interesting changes in materials, including interfacial bonding, charge injection barriers, molecular orientation, and morphological changes in neat materials and blends. These changes can affect the stretchability and electroluminescent properties of PLEDs. Therefore, there are plenty of parameters to adjust to optimize the performance of the stretchable PLEDs. Meanwhile, these devices should also provide unique opportunities to investigate the materials properties *in situ*.

METHODS

Raw Materials. AgNWs were synthesized according to a reported procedure.[5,56] GO was prepared from graphite by the modified Hummers method.[44,46] Siliconized urethane acrylate oligomer (UA) and an ethoxylated bisphenol A dimethacrylate (EBA) were supplied by Sartomer. 2,2-Dimethoxy-2-phenylacetophenone (photoinitiator), anhydrous chlorobenzene, and polyethylenimine (PEI), 80% ethoxylated solution (35−40 wt % in H_2O, average M_w ~70 000), were all obtained from Sigma-Aldrich. Low conductivity poly(3,4-ethylenedioxythiophene):poly(styrenesulfonate) (PEDOT:PSS) (Clevios VP AI4083) was purchased from H.C. Starck Inc. The white-light-emitting polymer was provided by Cambridge Display Technology. 2-Methoxyethanol (99+%) was bought from Acros, and 1,3-bis[(4-*tert*-butylphenyl)-1,3,4-oxidiazolyl]phenylene (OXD-7) was obtained from Lumtech.

Preparation of GO-Soldered AgNW Networks. To fabricate the GO solution, GO powder was first dispersed in distilled water at the concentration of 2 mg/mL in an ultrasonic bath for 30 min. The GO/H_2O solution was diluted with isopropyl alcohol (IPA) to 1 mg/mL and sonicated for an additional 30 min at room temperature. A glass or PET substrate was placed flat on a drawdown machine. A dispersion of AgNW in IPA was drop-casted into a thin line at one end of the substrate and drawn down with a Meyer rod to spread the solution to form a uniform coating. Different AgNW densities of the AgNW network on substrate was controlled by the concentration of the AgNW dispersion being 0.3, 0.5, and 0.7 wt % to obtain AgNW network densities of 85 mg/m^2 (D1), 127 mg/m^2 (D2), and 170 mg/m^2 (D3), respectively. The as-prepared AgNW network on substrate was then soaked in a GO dispersion (optimized to 1 mg/mL concentration in water and IPA prepared[46]) for 5 min, rinsed with distilled water, and dried. The HT-annealed AgNW network was prepared by heating at 180 °C for 30 min after the Meyer rod coating on a drawdown machine.

Fabrication of Stretchable Composite Electrodes. The above GO-AgNW network and HT-AgNW network coated on release substrate were subsequently overcoated with a precursor solution containing 100 weight parts of UA, 20 parts of EBA, and 1 part of the photoinitiator.[49] The coatings were cured under UV at 2.5 W/cm^2 intensity and peeled off of the release substrate. The AgNW network was transferred as the conductive surface of the resulting transparent composite electrodes.

Fabrication of Stretchable White PLED. In a typical procedure, GO-AgNW/PUA composite electrodes were cleaned in an ultrasonic bath with detergent and distilled water for 30 min each. PEDOT:PSS was first spin-coated on a composite electrode at 4000 rpm for 60 s, baked at 70 °C for 20 min, and vacuum-dried. The dried PEDOT:PSS coating was approximately 120 nm thick, as measured on a Dektak profilometer. An emissive polymer layer was spin-coated on the PEDOT:PSS-coated electrode from a solution containing a white-light-emitting polymer and OXD-7 mixed at the weight ratio of 100:10 codissolved in chlorobenzene. The emissive layer was 100 nm thick. A solution of PEI in methoxyethanol (diluted by adding 2-methoxyethanol to 0.4 wt %) was spin-coated on another composite electrode at 5000 rpm for 60 s and dried in vacuum. The thickness of the PEI layer was around 5 nm. Finally, the PEI/composite electrode and the emissive polymer/PEDOT:PSS/composite electrode were laminated with the active materials facing each other and heated to 100 °C for 3 min. The lamination process was done in a glovebox protected with nitrogen, with oxygen, and moisture levels below 0.5 ppm.

Characterization Methods. Cyclic strain tests and cyclic bending−unbending tests were performed on a motorized linear stage with built-in controller (Zaber Technologies Inc.). A Keithley 2000 digital multimeter was used to monitor the resistance change. Strain and resistance data were recorded with a custom-made LabView code. All the electrical measurements for stretchable PLED were carried out in the glovebox. The current−voltage−light intensity curves for the stretchable PLEDs in original state were measured with a Keithley 2400 source meter and a calibrated silicon photodetector by sweeping the applied voltage from 0 to 21 V at 500 mV increments per step. The current density and brightness for the stretchable PLED under stretched state were measured utilizing a Keithley 2400 source meter and a photoresearch PR-655. All tests were carried out at room temperature. The transmittance spectra were recorded utilizing a Shimadzu UV-1700 spectrophotometer. Scanning electron microscopy was performed on a JEOL JSM-6701F scanning electron microscope.

Conflict of Interest: The authors declare no competing financial interest.

Acknowledgment. The work reported here was supported by the Air Force Office of Scientific Research (FA9550-12-1-0074). We thank Dr. Richard Wilson of Cambridge Display Technology, Ltd. for supplying the white-light-emitting polymer.

Supporting Information Available: Additional figures are provided. These include an SEM image of the GO-AgNW network, transmittance spectra of GO-soldered AgNW networks and HT-annealed AgNW networks on glass, transmittance spectra of GO-AgNW/PET, CIE coordinate diagram for stretchable PLED, and a video showing a PLED under stretching−releasing cycles. This material is available free of charge *via* the Internet at http://pubs.acs.org.

REFERENCES AND NOTES

1. Lee, S. K.; Kim, B. J.; Jang, H.; Yoon, S. C.; Lee, C.; Hong, B. H.; Rogers, J. A.; Cho, J. H.; Ahn, J. H. Stretchable Graphene Transistors with Printed Dielectrics and Gate Electrodes. *Nano Lett.* **2011**, *11*, 4642–4646.
2. Lipomi, D. J.; Tee, B. C. K.; Vosgueritchian, M.; Bao, Z. Stretchable Organic Solar Cells. *Adv. Mater.* **2011**, *23*, 1771–1775.
3. Lipomi, D. J.; Vosgueritchian, M.; Tee, B. C. K.; Hellstrom, S. L.; Lee, J. A.; Fox, C. H.; Bao, Z. Skin-like Pressure and Strain Sensors Based on Transparent Elastic Films of Carbon Nanotubes. *Nat. Nanotechnol.* **2011**, *6*, 788–792.
4. Park, K.; Lee, D.-K.; Kim, B.-S.; Jeon, H.; Lee, N.-E.; Whang, D.; Lee, H.-J.; Kim, Y. J.; Ahn, J.-H. Stretchable, Transparent Zinc

Oxide Thin Film Transistors. *Adv. Funct. Mater.* **2010**, *20*, 3577–3582.
5. Yu, Z.; Niu, X.; Liu, Z.; Pei, Q. Intrinsically Stretchable Polymer Light-Emitting Devices Using Carbon Nanotube–Polymer Composite Electrodes. *Adv. Mater.* **2011**, *23*, 3989–3994.
6. Filiatrault, H. L.; Porteous, G. C.; Carmichael, R. S.; Davidson, G. J. E.; Carmichael, T. B. Stretchable Light-Emitting Electrochemical Cells Using an Elastomeric Emissive Material. *Adv. Mater.* **2012**, *24*, 2673–2678.
7. Tahar, R. B. H.; Ban, T.; Ohya, Y.; Takahashi, Y. Tin Doped Indium Oxide Thin Films: Electrical Properties. *J. Appl. Phys.* **1998**, *83*, 2631–2645.
8. Cairns, D. R.; Witte, R. P.; Sparacin, D. K.; Sachsman, S. M.; Paine, D. C.; Crawford, G. P.; Newton, R. R. Strain-Dependent Electrical Resistance of Tin-Doped Indium Oxide on Polymer Substrates. *Appl. Phys. Lett.* **2000**, *76*, 1425–1427.
9. Lacour, S. P.; Chan, D.; Wagner, S.; Li, T.; Suo, Z. Mechanisms of Reversible Stretchability of Thin Metal Films on Elastomeric Substrates. *Appl. Phys. Lett.* **2006**, *88*, 204103.
10. Liu, K.; Sun, Y.; Liu, P.; Lin, X.; Fan, S.; Jiang, K. Cross-Stacked Superaligned Carbon Nanotube Films for Transparent and Stretchable Conductors. *Adv. Funct. Mater.* **2011**, *21*, 2721–2728.
11. Sekitani, T.; Noguchi, Y.; Hata, K.; Fukushima, T.; Aida, T.; Someya, T. A Rubberlike Stretchable Active Matrix Using Elastic Conductors. *Science* **2008**, *321*, 1468–1472.
12. Shin, M. K.; Oh, J.; Lima, M.; Kozlov, M. E.; Kim, S. J.; Baughman, R. H. Elastomeric Conductive Composites Based on Carbon Nanotube Forests. *Adv. Mater.* **2010**, *22*, 2663–2667.
13. Zhang, Y.; Sheehan, C. J.; Zhai, J.; Zou, G.; Luo, H.; Xiong, J.; Zhu, Y. T.; Jia, Q. X. Polymer-Embedded Carbon Nanotube Ribbons for Stretchable Conductors. *Adv. Mater.* **2010**, *22*, 3027–3031.
14. Zhu, Y.; Xu, F. Buckling of Aligned Carbon Nanotubes as Stretchable Conductors: A New Manufacturing Strategy. *Adv. Mater.* **2012**, *24*, 1073–1077.
15. Geng, H. Z.; Kim, K. K.; So, K. P.; Lee, Y. S.; Chang, Y.; Lee, Y. H. Effect of Acid Treatment on Carbon Nanotube-Based Flexible Transparent Conducting Films. *J. Am. Chem. Soc.* **2007**, *129*, 7758–7759.
16. Bae, S.; Kim, H.; Lee, Y.; Xu, X.; Park, J. S.; Zheng, Y.; Balakrishnan, J.; Lei, T.; Kim, H. R.; Song, Y. I.; *et al.* Roll-to-Roll Production of 30-Inch Graphene Films for Transparent Electrodes. *Nat. Nanotechnol.* **2010**, *5*, 574–578.
17. Hecht, D. S.; Hu, L.; Irvin, G. Emerging Transparent Electrodes Based on Thin Films of Carbon Nanotubes, Graphene, and Metallic Nanostructures. *Adv. Mater.* **2011**, *23*, 1482–1513.
18. Kim, K. S.; Zhao, Y.; Jang, H.; Lee, S. Y.; Kim, J. M.; Kim, K. S.; Ahn, J. H.; Kim, P.; Choi, J. Y.; Hong, B. H. Large-Scale Pattern Growth of Graphene Films for Stretchable Transparent Electrodes. *Nature* **2009**, *457*, 706–710.
19. Kim, R. H.; Bae, M. H.; Kim, D. G.; Cheng, H.; Kim, B. H.; Kim, D. H.; Li, M.; Wu, J.; Du, F.; Kim, H. S.; *et al.* Stretchable, Transparent Graphene Interconnects for Arrays of Microscale Inorganic Light Emitting Diodes on Rubber Substrates. *Nano Lett.* **2011**, *11*, 3881–3886.
20. Argun, A. A.; Cirpan, A.; Reynolds, J. R. The First Truly All-Polymer Electrochromic Devices. *Adv. Mater.* **2003**, *15*, 1338–1341.
21. Lipomi, D. J.; Lee, J. A.; Vosgueritchian, M.; Tee, B. C. K.; Bolander, J. A.; Bao, Z. Electronic Properties of Transparent Conductive Films of PEDOT:PSS on Stretchable Substrates. *Chem. Mater.* **2012**, *24*, 373–382.
22. Vosgueritchian, M.; Lipomi, D. J.; Bao, Z. Highly Conductive and Transparent PEDOT:PSS Films with a Fluorosurfactant for Stretchable and Flexible Transparent Electrodes. *Adv. Funct. Mater.* **2012**, *22*, 421–428.
23. Lee, P.; Lee, J.; Lee, H.; Yeo, J.; Hong, S.; Nam, K. H.; Lee, D.; Lee, S. S.; Ko, S. H. Highly Stretchable and Highly Conductive Metal Electrode by Very Long Metal Nanowire Percolation Network. *Adv. Mater.* **2012**, *24*, 3326–3332.
24. De, S.; Higgins, T. M.; Lyons, P. E.; Doherty, E. M.; Nirmalraj, P. N.; Blau, W. J.; Boland, J. J.; Coleman, J. N. Silver Nanowire Networks as Flexible, Transparent, Conducting Films: Extremely High DC to Optical Conductivity Ratios. *ACS Nano* **2009**, *3*, 1767–1774.
25. Gaynor, W.; Lee, J. Y.; Peumans, P. Fully Solution-Processed Inverted Polymer Solar Cells with Laminated Nanowire Electrodes. *ACS Nano* **2010**, *4*, 30–34.
26. Hu, L.; Kim, H. S.; Lee, J. Y.; Peumans, P.; Cui, Y. Scalable Coating and Properties of Transparent, Flexible, Silver Nanowire Electrodes. *ACS Nano* **2010**, *4*, 2955–2963.
27. Lee, J.; Lee, I.; Kim, T. S.; Lee, J. Y. Efficient Welding of Silver Nanowire Networks without Post-processing. *Small* **2013**, *9*, 2887–2894.
28. Garnett, E. C.; Cai, W.; Cha, J. J.; Mahmood, F.; Connor, S. T.; Christoforo, M. G.; Cui, Y.; McGehee, M. D.; Brongersma, M. L. Self-Limited Plasmonic Welding of Silver Nanowire Junctions. *Nat. Mater.* **2012**, *11*, 241–249.
29. Chen, R.; Das, S. R.; Jeong, C. W.; Khan, M. R.; Janes, D. B.; Alam, M. A. Co-percolating Graphene-Wrapped Silver Nanowire Network for High Performance, Highly Stable, Transparent Conducting Electrodes. *Adv. Funct. Mater.* **2013**, *23*, 5150–5158.
30. Yu, Z.; Li, L.; Zhang, Q.; Hu, W.; Pei, Q. Silver Nanowire–Polymer Composite Electrodes for Efficient Polymer Solar Cells. *Adv. Mater.* **2011**, *23*, 4453–4457.
31. Yu, Z.; Zhang, Q.; Li, L.; Chen, Q.; Niu, X.; Liu, J.; Pei, Q. Highly Flexible Silver Nanowire Electrodes for Shape-Memory Polymer Light-Emitting Diodes. *Adv. Mater.* **2011**, *23*, 664–668.
32. Gaynor, W.; Burkhard, G. F.; McGehee, M. D.; Peumans, P. Smooth Nanowire/Polymer Composite Transparent Electrodes. *Adv. Mater.* **2011**, *23*, 2905–2910.
33. Tokuno, T.; Nogi, M.; Karakawa, M.; Jiu, J.; Thi Thi, N.; Aso, Y.; Suganuma, K. Fabrication of Silver Nanowire Transparent Electrodes at Room Temperature. *Nano Res.* **2011**, *4*, 1215–1222.
34. Yang, L.; Zhang, T.; Zhou, H.; Price, S. C.; Wiley, B. J.; You, W. Solution-Processed Flexible Polymer Solar Cells with Silver Nanowire Electrodes. *ACS Appl. Mater. Interfaces* **2011**, *3*, 4075–4084.
35. Feng, X. Y. Zhu. Highly Conductive and Stretchable Silver Nanowire Conductors. *Adv. Mater.* **2012**, *24*, 5117–5122.
36. Ge, J.; Yao, H. B.; Wang, X.; Ye, Y. D.; Wang, J. L.; Wu, J. Y.; Liu, J. W.; Fan, F. J.; Gao, H. L.; Zhang, C. L.; *et al.* Stretchable Conductors Based on Silver Nanowires: Improved Performance through a Binary Network Design. *Angew. Chem., Int. Ed.* **2013**, *52*, 1654–1659.
37. Yun, S.; Niu, X.; Yu, Z.; Hu, W.; Brochu, P.; Pei, Q. Compliant Silver Nanowire–Polymer Composite Electrodes for Bistable Large Strain Actuation. *Adv. Mater.* **2012**, *24*, 1321–1327.
38. Hu, W.; Niu, X.; Zhao, R.; Pei, Q. Elastomeric Transparent Capacitive Sensors Based on An Interpenetrating Composite of Silver Nanowires and Polyurethane. *Appl. Phys. Lett.* **2013**, *102*, 083303.
39. Hu, W.; Niu, X.; Li, L.; Yun, S.; Yu, Z.; Pei, Q. Intrinsically Stretchable Transparent Electrodes Based on Silver-Nanowire-Crosslinked-Polyacrylate Composites. *Nanotechnology* **2012**, *23*, 344002.
40. Moon, I. K.; Kim, J. I.; Lee, H.; Hur, K.; Kim, W. C.; Lee, H. 2D Graphene Oxide Nanosheets as an Adhesive Over-Coating Layer for Flexible Transparent Conductive Electrodes. *Sci. Rep.* **2013**, *3*, 1112.
41. Lee, J.; Lee, P.; Lee, H. B.; Hong, S. K.; Lee, I.; Yeo, J.; Lee, S. S.; Kim, T. S.; Lee, D. J.; Ko, S. H. Room-Temperature Nanosoldering of a Very Long Metal Nanowire Network by Conducting-Polymer-Assisted Joining for a Flexible Touch-Panel Application. *Adv. Funct. Mater.* **2013**, *23*, 4171–4176.
42. Suh, Y.; Lu, N.; Lee, S. H.; Chung, W.-S.; Kim, K.; Kim, B.; Ko, M. J.; Kim, M. J. Thin Ag Layer Induced by Poly(3,4ethylenedioxythiophene):Polystyrene Sulfonate in a Transmission Electron Microscopy Specimen of an Inverted Polymer Solar Cell. *ACS Appl. Mater. Interfaces* **2012**, *4*, 5118–5124.

43. Lee, M. S.; Lee, K. S.; Kim, S. Y.; Lee, H. J.; Park, J. H.; Choi, K. H.; Kim, H. K.; Kim, D. G.; Lea, D. Y.; Nam, S. W.; *et al.* High-Performance, Transparent, and Stretchable Electrodes Using Graphene−Metal Nanowire Hybrid Structures. *Nano Lett.* **2013**, *13*, 2814–2821.
44. Dikin, D. A.; Stankovich, S.; Zimney, E. J.; Piner, R. D.; Dommett, G. H. B.; Evmenenko, G.; Nguyen, S. T.; Ruoff, R. S. Preparation and Characterization of Graphene Oxide Paper. *Nature* **2007**, *448*, 457–460.
45. Gomez-Navarro, C.; Burghard, M.; Kern, K. Elastic Properties of Chemically Derived Single Graphene Sheets. *Nano Lett.* **2008**, *8*, 2045–2049.
46. Liang, J.; Huang, Y.; Zhang, L.; Wang, Y.; Ma, Y.; Guo, T.; Chen, Y. Molecular-Level Dispersion of Graphene into Poly(vinyl alcohol) and Effective Reinforcement of Their Nanocomposites. *Adv. Funct. Mater.* **2009**, *19*, 2297–2302.
47. Suk, J. W.; Piner, R. D.; An, J.; Ruoff, R. S. Mechanical Properties of Monolayer Graphene Oxide. *ACS Nano* **2010**, *4*, 6557–6564.
48. Ahn, Y.; Jeong, Y.; Lee, Y. Improved Thermal Oxidation Stability of Solution-Processable Silver Nanowire Transparent Electrode by Reduced Graphene Oxide. *ACS Appl. Mater. Interfaces* **2012**, *4*, 6410–6414.
49. Liang, J. J.; Li, L.; Niu, X. F.; Yu, Z. B.; Pei, Q. B. Elastomeric Polymer Light-Emitting Devices and Displays. *Nat. Photonics* **2013**, *7*, 817–824.
50. Chun, K.-Y.; Oh, Y.; Rho, J.; Ahn, J.-H.; Kim, Y.-J.; Choi, H. R.; Baik, S. Highly Conductive, Printable and Stretchable Composite Films of Carbon Nanotubes and Silver. *Nat. Nanotechnol.* **2010**, *5*, 853–857.
51. Lu, N. S.; Wang, X.; Suo, Z. G.; Vlassak, J. Metal Films on Polymer Substrates Stretched Beyond 50%. *Appl. Phys. Lett.* **2007**, *91*, 221909.
52. Sun, Q.; Li, Y.; Pei, Q. Polymer Light-Emitting Electrochemical Cells for High-Efficiency Low-Voltage Electroluminescent Devices. *J. Disp. Technol.* **2007**, *3*, 211–224.
53. Yu, Z.; Li, L.; Gao, H.; Pei, Q. Polymer Light-Emitting Electrochemical Cells: Recent Developments To Stabilize the p-i-n Junction and Explore Novel Device Applications. *Sci. China: Chem.* **2013**, *56*, 1075–1086.
54. Zhou, Y. H.; Fuentes-Hernandez, C.; Shim, J.; Meyer, J.; Giordano, A. J.; Li, H.; Winget, P.; Papadopoulos, T.; Cheun, H.; Kim, J.; *et al.* Universal Method To Produce Low-Work Function Electrodes for Organic Electronics. *Science* **2012**, *336*, 327–332.
55. Matyba, P.; Yamaguchi, H.; Eda, G.; Chhowalla, M.; Edman, L.; Robinson, N. D. Graphene and Mobile Ions: The Key to All-Plastic, Solution-Processed Light-Emitting Devices. *ACS Nano* **2010**, *4*, 637–642.
56. Sun, Y. G.; Gates, B.; Mayers, B.; Xia, Y. N. Crystalline Silver Nanowires by Soft Solution Processing. *Nano Lett.* **2002**, *2*, 165–168.